

Design and analysis of the mechanical structure of a linear micromotor based on CMOS-MEMS technology

Andrea López-Tapia
Electrical Engineering Dept.
CINVESTAV-IPN
Mexico City, Mexico
andrea.lopez@cinvestav.mx

Mario Alfredo Reyes-Barranca
Electrical Engineering Dept.
CINVESTAV-IPN
Mexico City, Mexico
mreyes@cinvestav.mx

Griselda Stephany Abarca-Jiménez
UNIDAD PROFESIONAL INTERDISCIPLINARIA CAMPUS HIDALGO INSTITUTO POLITÉCNICO NACIONAL
Hidalgo, 42162, Mexico
Mexico City, Mexico
gabarcaj@ipn.mx

Luis Sánchez-Márquez
Electrical Engineering Dept.
CINVESTAV-IPN
Mexico City, Mexico
luis.sanchez.m@cinvestav.mx

Luis Martín Flores-Nava
Electrical Engineering Dept.
CINVESTAV-IPN
Mexico City, Mexico
lmflores@cinvestav.mx

Oliverio Arellano-Cárdenes
Electrical Engineering Dept.
CINVESTAV
Mexico City, Mexico
arellano@cinvestav.mx

Abstract— This paper shows the design of the mechanical structure of a linear electrostatic micromotor, consisting on four springs to which a moving set of electrodes (which will move due to the electrostatic actuation) is attached to, together with one of the plates for a position sensor of the system. This structure is designed in an aluminum layer under the rules of the standard CMOS technology. In addition, the mechanical structure model which is presented, eliminates the friction between it and the substrate. The simulations were obtained using COMSOL.

Keywords—MEMS, Linear Micromotor, Mechanical Structure, Electrostatic Actuation

I. INTRODUCTION

Since its appearance in the 1980s, the microelectromechanical systems (MEMS) have had a continuous and extensive development. Technology and research have advanced in the area of micromachining, this has allowed the design of more complex and novel devices. In this work we have paid special attention to the linear micromotors MEMS, which are actuators characterized by dimensions in ranges from submillimeters to millimeters and have a very important role in micro-scale devices.

Some of its immediate applications would be in miniaturized robotics and other machines such as micropistons or electrovalves; for example, it could be applied into medical instruments such as microvalve control [1].

Based on this background, it can be stated that there are very few designs of micromotors compatible with the standard CMOS technology, which is of vital importance for an

application, since both the mechanical structure and the control circuit would be within the same chip, therefore both the area occupied by the entire system and its cost are reduced. The development that was made in the present work shows one of the parts that constitute a linear micromotor, which is the mechanical structure.

II. LINEAR MICROMOTOR MEMS

The driving forces for micromotors are primarily of electrostatic nature. The tangential force generated in pairs of misaligned electrically energized plates, provides the required movement in a linear motor [2].

Fig.1 illustrates the operating principle of the linear movement between two sets of parallel plates. Each set of plates contains a number of electrodes made of conductive material.

The mobile electrodes are positioned in a linear manner with a constant spacing between them, in such a way that they are out of phase with the fixed electrodes. The fixed electrodes are positioned in a linear manner in front of the movable ones with a constant separation. Therefore, when a potential difference between both electrodes is applied, an electrostatic force moves the motor one step horizontally. This phenomenon is reproduced again in the next pair of electrodes to move the motor another step and so on until reaching the final position.

The parts that constitute the linear micromotor system designed under the rules of the standard CMOS technology are shown in Fig.2 and they are: the control circuit, the mechanical

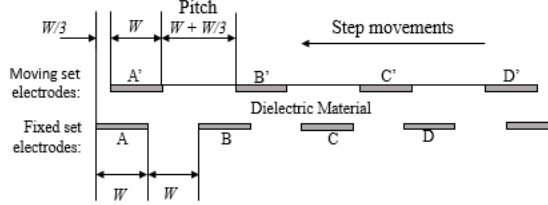


Fig. 1. Principle of operation of electrostatic micromotors.

structure and the position sensor. However, this paper focuses on the mechanical structure.

A. Micromechanical springs

A contribution of the presented proposal, is the use of springs as a support of the mobile electrodes, which is not common in this type of devices. These springs will have the function of supporting the arrangement of capacitive plates and guiding them in the moving axis, as well. The springs are a basic construction structure for many micromechanical devices. The MEMS spring design is relatively simple and combines some standard structures. The springs that are more complex can be analyzed as combinations of basic shapes that can be configured either in series, in parallel or in mixed form. The more accuracy is desired, the more it will be necessary to refine the results by numerical simulations such as a finite element analysis. This behavior will be presented later.

III. DESIGN OF THE MECHANICAL STRUCTURE

One of the most important issues or problems in the design of the structures of a micromotor is how to reduce the friction and surface sticking between the moving part and the substrate [3]. In motors made in other works, there is a contact between the moving part and the lower layers; this surface contact result in a relatively large friction for the micromotor, which contributes to increasing motor wear and therefore reducing its life.

To avoid this friction, it is possible to have an arrangement of springs at each end of the actuator shown in Fig.1. Hence, the structure is suspended on the air and the force that must be overcome is that necessary to move the springs and not that due to friction. Consequently, and from the electrostatic point of view, it will be necessary to calculate the force required to move the springs and then the voltage (V_{motor}) to obtain this force.

A. Material of the springs and their deflection

The layer in which the springs and the actuator will be manufactured is Metal 1 (aluminum) having a thickness (h) of $0.64\mu m$. To define the dimensions of the springs, it is necessary to analyze their deflection. If there is such a deformation that the distance between Metal 1 and Poly 1 is modified, then the sensor measurements will be modified, as well as an increase in the risk of non-overlapping between the electrodes will be latent as shown in Fig.3, where W is the width of the electrode, h its thickness, d the separation between electrodes and F_e is the electric force. To obtain the electric force (1) is used [4], where ϵ is the permittivity of air and n is the number of pairs of electrodes that are activated at the same time. If there is no overlap between the electrodes, they will not interact with each other and the electric force will not manifest.

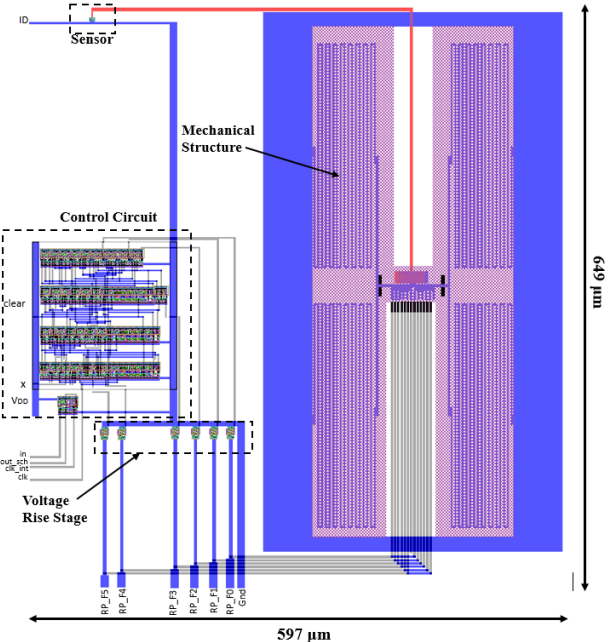


Fig. 2. Topological design of the linear micromotor system.

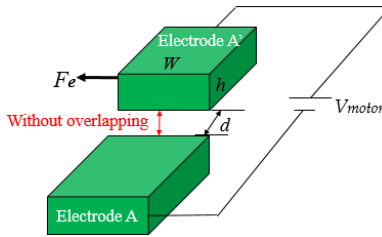


Fig. 3. Electrodes without overlap.

$$F_e = n \frac{1}{2} \frac{\epsilon h}{d} V_{motor}^2 \quad (1)$$

The springs are composed of a certain number of beams joined together; these beams are connected in series as shown in Fig.4, where L_y is the length of each beam, w is the width of each beam, and L_u is the separation between each beam.

To calculate the deflection of the springs, it is first considered that the structure is symmetrical, and that only one of the ends is required to analyze. A second consideration is that the spring is ideally a uniform bar fixed at one end, and that it loads half of the weight of the mobile structure of the motor at the other end, then it can be idealized as a cantilever beam as shown in Fig.5.

To obtain the deflection at the end of the beam, (2) is used [4], which gives us the displacement along the y-axis, where the moment of inertia of each beam is given by $I = ah^3/12$. The force is given by half the weight of the actuator due to the symmetry of the structure $F = mg/2$. The mass of the actuator is given by $m = \rho Vol$, where ρ is the density of Metal 1 and the volume is given by $Vol = A_{act}h$, where A_{act} is the value of the area

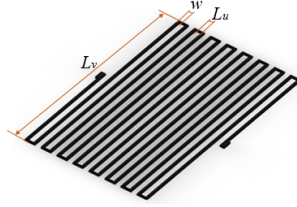


Fig. 4. Simple spring configuration.

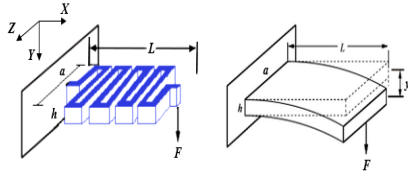


Fig. 5. Spring deflection and idealization.

of the actuator that includes the supports. From the previous equations, some constants are shown in TABLE I.

$$y = \frac{L^3 F}{3EI} \quad (2)$$

Using all the previous equations the graph to study the deflection of the springs, is obtained. In Fig.6 it can be seen that if the length L increases, so does the deflection. In contrast, if the length a increases, the deflection is smaller, and the force required to displace the spring in the x -axis direction is smaller. Hence it is decided to use an arrangement of two springs in parallel (see Fig.7) to make the length a longer, but without making the length of each beam L_v longer, this prevents deformation of the springs or from breaking during the micromachining step.

B. Electric force and voltage

On the other side, in order to move the motor as explained in section II, it is necessary an electric force (F_e) to displace a pair of electrodes and this force is given by (1). However, in the design, it is also necessary to make a calculation of the force required to move the springs. Therefore, considering all the forces present in the system will require the analysis of an equilibrium system like that shown in Fig.8.

TABLE I. CONSTANTS USED FOR DEFLECTION CALCULATION

Parameter	Value
Metal 1 Thickness (h)	0.64 μm
Young's modulus of Metal 1/ Aluminum (E)	70 GPa
Actuator area (A_{act})	$2.23 \cdot 10^3 \mu\text{m}^2$ [5]
Actuator volume (Vol)	$1.42 \cdot 10^{-3} \mu\text{m}^3$ [5]
Metal 1 density (ρ)	2700 Kg/m ³
Gravity (g)	9.81 m/s ²
Force due to weight (F)	$18.92 \cdot 10^{-18} \text{ N}$

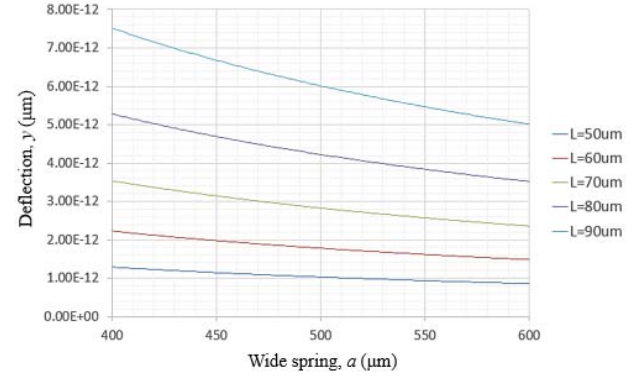


Fig. 6. Deflection graph.

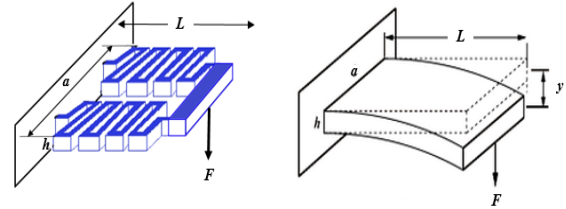


Fig. 7. Deflection of a pair of springs in parallel.

In this diagram it can be observed that the electric force necessary to move the whole structure must counteract the forces that oppose the movement, which are the sum of the forces (F_k) to displace each pair of springs that are at the ends of the actuator.

To obtain the force (F_k), the arrangement of springs in parallel shown in Fig.7, is analyzed; it can be considered that there are two identical springs composed of beams connected in series and both springs are connected in parallel, therefore the spring constant [4] of that arrangement is given by (3):

$$k = P \left(\frac{N}{k_{II}} \right)^{-1} \quad (3)$$

Where k_{II} is the spring stiffness constant of one of the beams that make up the spring that behave like a guided spring and is given by $k_{II} = 12EI_v/L_v^3$, where I_v is the moment of inertia of a beam given by $I_v = hw^3/12$, N is the number of beams and P is the number of springs in parallel. Finally, to obtain the total force due to the four springs, it is necessary to clarify that the springs move an amount δ for each step and the force of each pair of springs is given by $F_k = k\delta$, so the sum of the forces due to the two pairs of springs, is given by (4).



Fig. 8. Force diagram.

$$F_{k\text{tot}} = 2k\delta \quad (4)$$

Making equal (1) and (4) since $F_e = F_{k\text{tot}}$, it is possible to obtain the voltage that must be applied to each pair of electrodes (5), such that they can move to get aligned, where n is the total number of active pair electrodes, $\epsilon = \epsilon_R \epsilon_0$ is the permittivity of air, h is the thickness of an electrode.

$$V_{\text{motor}} = \sqrt{\frac{2F_{k\text{tot}}d}{n\epsilon h}} \quad (5)$$

Since the motor consists of 13 fixed electrodes and 12 mobile electrodes, that is, two pairs of electrodes are activated at the same time as shown in Fig.9, for example the red electrodes that are two pairs of electrodes, are activated at the same time, then the value that should be considered for n in (2) must be two. There could be more electrode pairs, but it should be considered that for each pair added, means six more pairs to achieve sequential movement while corresponding plates overlap. This will increase the size and weight of the motor, modifying the force necessary to move it.

Another aspect that must be taken into consideration with regard to the springs is the separation between each beam (L_u) [6]. From the technological standpoint, to have a better penetration of the chemical etching solution through the structure of the spring, during the micromachining step, it is necessary to leave separations with a minimum width of 10λ (λ is the scaling factor of the device dimensions), that is, $3\mu\text{m}$ since in the $0.5\mu\text{m}$ technology one λ is equal to $0.3\mu\text{m}$.

Considering the above, power and voltage graphs were made to choose the final value of all the parameters shown in Fig.3, from where a suitable operating trade-off can be chosen.

Figs.10a) and 10b) show the graphs of the behavior of the total force required to move the springs as well as the voltage, as a function of the width of the spring beams (w), respectively. Besides, a parametric sweep was made with different number of beams in a spring, resulting that both, $F_{k\text{tot}}$ and V_{motor} , decrease.

On the other hand, and following the required geometry of the springs, for the width of the beams of the springs, the design rules [7] must be respected. From this, the beams must have a minimum width of 3λ , therefore it is chosen a value of $1.2\mu\text{m}$, that is 4λ and thus there is less risk of breakage and as observed in the previous graphs, with this value both the force and the voltage are lower, which is the objective.

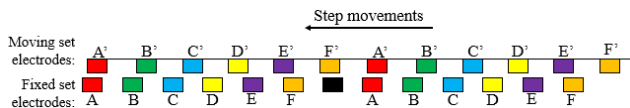


Fig. 9. Electrodes distribution in the motor.

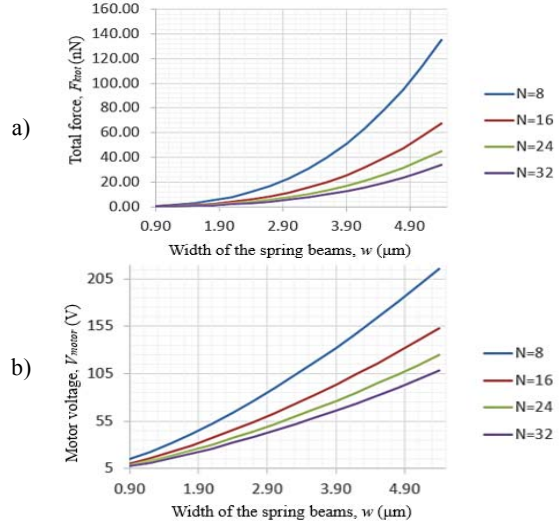


Fig. 10. a) Graph $F_{k\text{tot}}-w$, b) Graph $V_{\text{motor}}-w$.

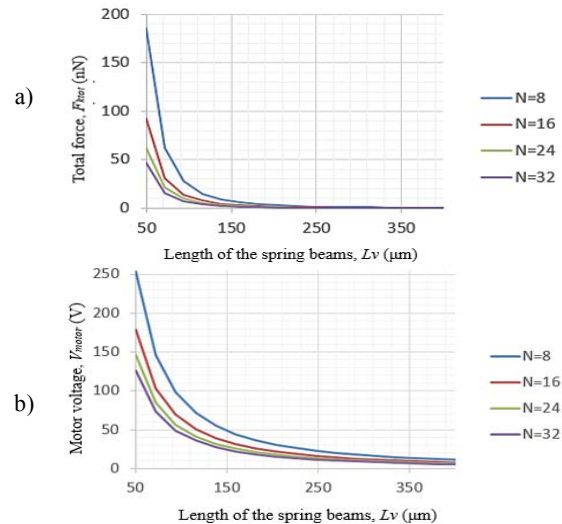


Fig. 11. a) Graph $F_{k\text{tot}}-L_v$, b) Graph $V_{\text{motor}}-L_v$.

Then, in Figs.11a) and 11b) the graphs of the behavior of the total force as well as the voltage are shown, as a function of the length of the spring beams (L_v), performing also a parametric sweep of the number of beams in a spring, which shows that as the number of beams grow, $F_{k\text{tot}}$ and V_{motor} decrease.

Therefore, it can be concluded that a decrease in $F_{k\text{tot}}$ and V_{motor} will be achieved if the length of the beams is increased, which is desirable to work with low values of voltage inside the chip. However, a compromise must be achieved in which the springs should not be too long or to reduce the risk of breaking during the release of the mobile structure and having a greater deflection, as well, as shown in the graph of deflection in Fig.6. Then, based on the above, a value of L_v of $250\mu\text{m}$ is chosen, therefore the value a in the deflection (2) would be $540\mu\text{m}$ counting twice L_v and a separation between springs of $40\mu\text{m}$.

A graph showing how the total force and voltage varies with the width of the electrodes (W) is shown in Figs.12a) and 12b), with a parametric sweep of the number of beams in a spring (N),

which shows that when the number of beams increases, both F_{ktot} and V_{motor} will decrease.

From the previous analysis, it can be concluded that the wider the electrodes are, the bigger F_{ktot} and V_{motor} will be. In this case it is worth commenting that by design rules of the technology on which this proposed design is based, the width of the electrode (W) cannot be less than 3λ , therefore a value of W of $1.8\mu\text{m}$, that is 6λ is selected, then the value of each step of the motor will be $0.6\mu\text{m}$.

Finally, Fig.13 shows the behavior of the voltage required to move the entire structure as a function of the distance (d) separating each pair of electrodes, as well as a parametric sweep of the number of beams in a spring.

What it can be seen from the graph in Fig.13, is that with a shorter distance there will be a better behavior, however the effect of air conductivity between the plates must be avoided and with this in mind, a value of $1.95\mu\text{m}$ is chosen.

Based on all the previous graphs, it can be seen that the greater the number of beams, the lower the force and the lower the voltage will result. However, this also implies greater deflection; therefore, an intermediate number of 16 beams is chosen for the final design. Finally, the dimensions of the springs and some dimensions of the electrodes are shown in TABLE II.

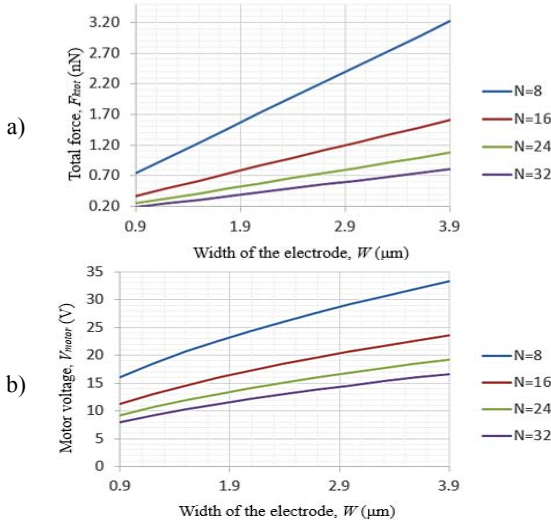


Fig. 12. a) Graph F_{ktot} - W , b) Graph V_{motor} - W .

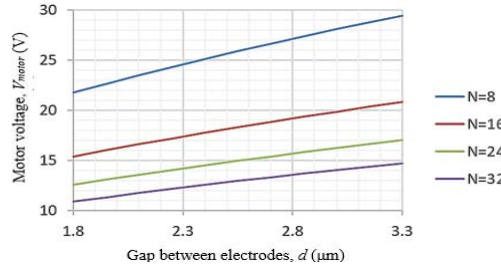


Fig. 13. Graph V_{motor} - d .

TABLE II. FINAL PARAMETERS

Parameter	Value
Number of beams (N)	16
Beam width (w)	$1.2\mu\text{m}$
Beam lenght (L_v)	$250\mu\text{m}$
Union lenght(L_u)	$3\mu\text{m}$
Electrode width (W)	$1.8\mu\text{m}$
Motor step($W/3=\delta$)	$0.6\mu\text{m}$
Separation between plates (d)	$1.95\mu\text{m}$

With the parameters shown in TABLE II it can be obtained the value of the total force to move the springs (F_{ktot}) of 371.6 pN and the voltage (V_{motor}) that must be applied to the electrodes to move the motor will be 16V . The resulting structure is shown in Fig.14, with the previously proposed dimensions, in addition to small stops or guides, which limit their movement in the z-axis direction and they will also serve to prevent the fixed electrodes from sticking with the mobiles.

IV. RESULTS

The main objective of the mechanical design is to anticipate the performance of the system prior to its fabrication through a CMOS foundry, so it is convenient and necessary to use more complete tools to simulate and analyze microsystems with complex components and geometries. In the mechanical and electromechanical simulations that will be presented below, the software COMSOL is used, which implements the finite element analysis.

A. Deflection simulation of the springs

The role of the gravitational force on the weight of the structure of the springs that support the mobile electrodes is considered, in order to verify that there will be no misalignment of the structural layers that make up the electrostatic capacitor, since if this happens, it would prevent from the proper operation of the micromotor. Using COMSOL, some conditions for the analysis of the piece are defined: two fixed ends (its movement is limited in all the axes) shown in Fig.15, the force due to the weight of the entire structure by the action of gravity in the

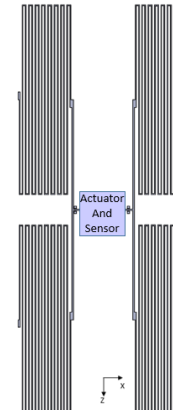


Fig. 14. Mechanical structure of the micromotor.

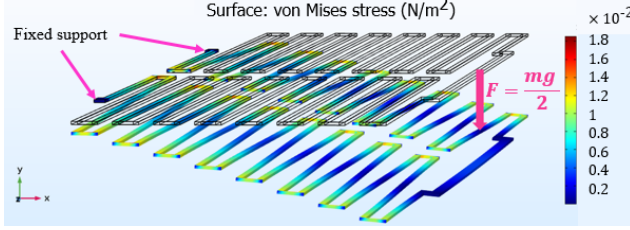


Fig. 15. Deflection simulation of a pair of springs.

-y-axis direction and the force that is applied due to half the weight of the actuator in the -y-axis direction as shown in Fig.15.

As shown in Fig.16 there is a deformation of the structure in which the maximum Von Mises stress has an approximate value of 20mPa, and since this value does not exceed the Young's modulus of the layer material (Metal 1) which is 70GPa, then the structure will not experience permanent deformations and there is a low probability of ruptures.

Finally, we obtain a displacement in the -y-axis direction of $1.08 \times 10^{-7} \mu\text{m}$, this is the value of the deflection due to the gravitational force. This value is considered small compared to the separation between the layers of Poly 1 and Metal 1 which is $1.137 \mu\text{m}$. Therefore, it demonstrates that the faces of the layers forming the parallel plates of the electrostatic capacitor will still have an overlap and the desired phenomenon for the operation of the micromotor can be yet present despite the presence of the gravitational force.

B. Displacement simulation of the springs

Now, with regard to the physical resistance of the structural layer from which the springs are made (aluminum-Metal 1), the result is presented when a force is applied, simulating the maximum mechanical stimulus considered, to evaluate the strength of the material. This force will be the one that will lead to move the springs to the maximum distance for which the system is being designed. Then, using COMSOL, the following conditions are defined in order to make the analysis of the piece: two fixed ends (its movement is limited in all the axes), and the electrostatic force applied will have a value of 371.6 pN , remembering that it is necessary to move the motor one step ($0.6 \mu\text{m}$) when $16V$ is applied, as shown in Fig.16.

After considering the above conditions for simulation and as is shown in Fig.16 there is a deformation of the structure in which the maximum Von Mises stress resulted in a value of 200 kPa . Since this value does not exceed the Young's modulus of the material layer (Metal 1), that is 70 GPa , then the structure will not suffer permanent deformations and there is a low probability of ruptures.

Finally, a displacement in the x-axis direction of $0.612365 \mu\text{m}$ is obtained as shown in Fig.17, which shows that by applying a potential difference of $16V$ between the electrodes, the value of one-step displacement of the motor gave $0.6 \mu\text{m}$ according to the specifications of the proposed design.

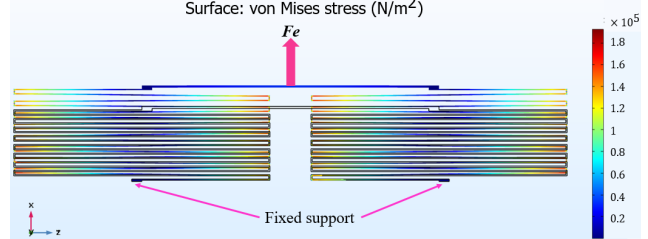


Fig. 16. Displacement simulation of a pair of springs.

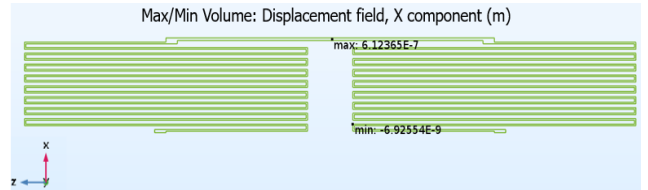


Fig. 17. Maximum and minimum displacement in x-axis direction of a pair of springs.

V. CONCLUSIONS

Based on all the micromotors found in different bibliographies, it was found that the existing designs have displacement limitation; however, the design of this linear micromotor has freedom of displacement due to the distribution of its electrodes. Another advantage of this design is its compatibility with the manufacturing technology of standard CMOS integrated circuits, in which the topological design of the control circuit, the position sensor and the mechanical structure could be realized. It was possible to integrate in the same substrate a MEMS device with the control circuit and the sensor stage, using the same design rules of the 0.5 micron CMOS technology of On Semiconductor.

Taking into account the results obtained from the analysis of the mechanical structure, it can be concluded that it has enough rigidity so as not to deform in a way that affects the operation of the micromotor.

REFERENCES

- [1] AMETEK, "FAQ," 2017. [Online]. Available: <https://www.haydonkerkpitman.com>. [Accessed Abril 2018].
- [2] T.-R. Hsu, MEMS and Microsystems: Design and Manufacture, Mc Graw Hill, 2002.
- [3] D. Barbade, "Micromotor fabrication by surface micromachining technique," *MEMS and nanotechnology*, vol. 2, 2010.
- [4] V. Kaajakari, Practical MEMS, Las Vegas, Nevada: Small Gear Publishing, 2009.
- [5] A. Lopez-Tapia, *Análisis y diseño de un micromotor lineal basado en tecnología CMOS-MEMS*, México, 2018.
- [6] G. S. Abarca-Jiménez, Sistema electrónico para un acelerómetro empleado FGMOs para correlación de parámetro inercial, Mexico City, 2016.
- [7] O. Semiconductor, "C5X 0.5 Micron Technology Design_Rules," 2011.